CHLOROPLAST SEQUESTRATION BY BENTHIC FORAMINIFERS IN DEEP-SHELF SEDIMENTS OF THE HIGH ARCTIC

Joan M. Bernhard^{1,*}, Emmanuelle Geslin², Magali Schweizer², Christiane Schmidt^{2,3,4}, Charlotte LeKieffre⁵
AND Giuliana Panieri^{6,7}

ABSTRACT

While foraminiferan protists (single-celled eukaryotes) inhabit a wide variety of habitats and have been doing so for hundreds of millions of years, we still do not fully understand their physiological capabilities. One rather unusual attribute is the ability of certain benthic foraminifera to sequester chloroplasts, which are the photosynthetic organelle of (other) eukaryotes. Such "kleptoplasty" has been documented in approximately 20 foraminifera species, mostly from shallow-water habitats such as mudflats where sunlight is readily available. Kleptoplasty in deeper-water benthic foraminifers is less commonly documented. Sediment cores collected via ROV in 2018 from a ~380-m deep area off southern Svalbard were sourced for living benthic foraminifera. Foraminifera were identified using DNA barcoding. Using Transmission Electron Microscopy (TEM) and subsequent cellular ultrastructural analysis, we established specimen viability and the presence of sequestered chloroplasts. Eukaryotic microbiomes of these four taxa were also sequenced to investigate the identity of the putative kleptoplast donors. The common benthic foraminifera Buccella sp., Elphidium clavatum (Phylotype Elphidium S4), Nonionellina labradorica, and Robertina arctica contained abundant structurally intact chloroplasts that appear to be of diatom origin based on morphology. While it is known that N. labradorica and some Elphidium species are kleptoplastidic, this is the first report of kleptoplasty for Buccella and Robertina, primary documentation of kleptoplastidic *Elphidium* living at >375-m water depth, and the first time kleptoplastidic N. labradorica has been noted in a microbial mat of a deep-water hydrocarbon seep. We believe R. arctica represents an unprecedented case of kleptoplasty in an aragonitic benthic foraminifera.

INTRODUCTION

The use of photosynthetic endosymbionts by both planktic and benthic foraminifera is rather common in both modern (e.g., Lee, 1995; Schiebel & Hemleben, 2017) and, presumably, ancient oceans (e.g., Norris et al., 2013; Takagi et al.,

 $^{\rm 1}$ Woods Hole Oceanographic Institution, Geology & Geophysics Department, Woods Hole, MA 02543, USA

2015). In these cases, the host foraminifer inhabits environments such as near-surface ocean waters or coral reefs where exposure to sunlight is generally attainable on a daily basis. The biological byproducts of the photosynthetic endosymbionts are assumed to benefit the host foraminifer (e.g., Hallock, 1999; LeKieffre et al., 2018c), presumably providing the ability to outcompete foraminifers that lack photosynthetic endosymbionts.

A specialized type of symbiosis, chloroplast sequestration, occurs in benthic foraminifera (Lopez, 1979; Pillet & Pawlowski, 2013; Bernhard & Geslin, 2018) but, to our knowledge, not in planktic foraminifera. In this type of association, only the photosynthetic organelle (chloroplast) is visible within the foraminifer's cytoplasm as opposed to an entire algal cell in the case of true endosymbiosis (Jauffrais et al., 2017). The specialized association between a eukaryotic host and chloroplasts from another eukaryote is often called "kleptoplasty", equating the chloroplast to a stolen item. The phenomenon occurs in protists such as foraminifera and ciliates (e.g., Stoecker et al., 2009; Johnson et al., 2023) but is far less common in metazoans, being documented only in particular gastropods (i.e., sacoglossan sea slugs; Jesus et al., 2010; Cartaxana et al., 2021) and in two species of Rhabdocoela flatworms (Van Steenkiste et al., 2019).

In general, the chloroplasts from diatoms comprise the majority of identified kleptoplasts in foraminifera. While only the chloroplast is visible in cytological preparations, it is usually possible to amplify diatom nuclear genes such as the 18S rDNA from shallow-water species of kleptoplastidic foraminifera (Jauffrais et al., 2019b; Schweizer et al., 2022) as well as those from deeper waters (Jauffrais et al., 2019a; Gomaa et al., 2021). Therefore, the diatom nucleus may be retained for some time before digestion (Jauffrais et al., 2019b).

A considerable number of shallow-water benthic foraminifera are known to sequester chloroplasts (Lopez, 1979; Jauffrais et al., 2018). Most of these host foraminifers inhabit shallow-water environments exposed to sunlight (Jauffrais et al., 2016, 2018, 2019b). It has been postulated that benthic foraminifera living in sunlit but oxygen-depleted habitats such as, for example, mudflats benefit from kleptoplasty (Cedhagen, 1991; Bernhard & Bowser, 1999; Cesbron et al., 2017; LeKieffre et al., 2018b) presumably because the chloroplast would provide oxygen to the host foraminifera.

Interestingly, kleptoplasty in benthic foraminifers from deeper waters, where sunlight is greatly attenuated, is also documented, although less often. For example, kleptoplastidic *Nonionellina labradorica* was documented as deep as 300-m water depth in Gullmar Fjord (Cedhagen, 1991). The closely related kleptoplastidic foraminifer *Nonionella stella* Cushman and Moyer, 1930, can be stunningly abundant deeper than 550 m in lowoxygen to anoxic sediments (Bernhard et al., 1997), occurring in numbers up to about two orders of magnitude greater than those of foraminifera in typical, aerated, marine sediments. The exact role of kleptoplasts in aphotic (dark) habitats, where

² Univ Angers, Nantes Université, Le Mans Univ, CNRS, Laboratoire de Planétologie et Géosciences, LPG UMR 6112, 49000 Angers, France

³ ZMT, Center for Tropical Marine Research, Fahrenheitstrasse 6, 28359 Bremen, Germany

⁴ TIB, Leibniz Information Centre for Science and Technology, 30167, Hannover, Germany, present address

⁵LPCV, IRIG, University of Grenoble, CEA, CNRS, INRAE, Grenoble, France

⁶ Department of Geoscience, UiT The Arctic University of Norway, Tromsø, Norway

⁷ CNR, ISP Institute of Polar Science, Campus Scientifico-Universitá Ca' Foscari Venezia, 30172 Mestre, Italy, present address

^{*} Correspondence author. E-mail: jbernhard@whoi.edu

photosynthesis cannot be fueled by sunlight, remains enigmatic (Bernhard & Bowser, 1999; Grzymski et al., 2002; Jauffrais et al., 2019a). Gene expression analyses have been useful for understanding the success of *N. stella* in this context (Gomaa et al., 2021; Powers et al., 2022; Gomaa et al., 2025). Here, we report the occurrence of sequestered chloroplasts in four species of benthic foraminifera collected from above the Arctic Circle (66°34'N) in water depths exceeding 375 m. To our knowledge, this is the first documentation of benthic foraminiferal kleptoplasty in the high Arctic.

The area investigated is the Storfjordrenna region off southern Svalbard (Norway; Fig. 1). The region has been studied due to, for example, its role in sea-ice formation (e.g., Fossile et al., 2020) and presence of many gas hydrate mounds (i.e., methane seeps; e.g., El Bani Altuna et al., 2021). This contribution is part of a larger project focused on biogeochemistry and history of methane emission sites in the Arctic (e.g., Gründger et al., 2019; Carrier et al., 2020; Yao et al., 2020). The bottom waters of the region are approximately 1°C (Bünz et al., 2022) and well aerated (e.g., >300 μ M L⁻¹; Fossile et al., 2020). The sediments are mostly clay and silty clay (Bünz et al., 2022). Profiles of dissolved oxygen indicate penetration to about 2 cm in non-seep areas of the region (Bünz et al., 2022).

Our samples were collected from two habitats in the vicinity of Gas Hydrate Pingo 3 (Hong et al., 2017, 2018) that is situated near the shelf-slope break (Fig. 1). The pingo has numerous bacterial mats, presumed to be sulfide-oxidizing bacterial mats, such as Beggiatoa or Arcobacter, that exhibited a dark/ black sediment near the surface (few mm) and strong smell of hydrogen sulfide (Bünz et al., 2022). The oxygen penetration depth (OPD) in these bacterial mats is around 1 mm (EG and D. Kalenitchenko, unpublished data). The sulfate-methane transition can be remarkably close to the sediment-water interface in these emission sites (e.g., <20 cm; Dessandier et al., 2020). Preliminary investigations of pore-water alkalinity conducted onboard during the cruise (Bünz et al., 2022) showed that microbial-mat microhabitats are associated with very high alkalinity compared to non-seep sediments, with steep gradients in the microbial mat sites from 0–5 cm below the seafloor. These trends are generated by intense anaerobic oxidation of methane releasing bicarbonate into pore water. The high alkalinity and profile shape suggest a sulfate-methane transition located at ~5 cm depth. This 'compressed' biogeochemical zonation is indeed typical of microbial-mat microhabitats at cold seeps (Angeles et al., 2025). Therefore, H2S fluxes toward the seafloor are expected to be high in microbial mats, and lower at non-seep areas.

In addition to microbial mat core collections indicative of active methane seepage, cores from sites not impacted by methane emissions were also recovered for comparative analyses. Our original aim was to compare cellular structure of conspecifics from seep vs. non-seep habitats to determine if symbionts or other adaptations were present in either or both of these populations.

MATERIALS AND METHODS

SAMPLING

Samples for this contribution were collected via the manipulator arm of the remotely operated vehicle (ROV) Ægir in

October 2018 on R/V Kronprins Haakon cruise CAGE18-05, off the southern tip of Svalbard (Norway). Benthic foraminifera were obtained from four sediment cores, two of which were pushcores and the others blade cores. All materials were collected from 379-383 m water depth (Figs. 1A, B). PUC2 and PUC34 were pushcores (8 cm inner diameter); BLC18 and BLC21 were blade cores (small boxcore; 20 × 12 cm surface area). PUC34, BLC18, and BLC21 were reference cores (nonseep controls), while PUC2 was collected in a microbial mat associated with methane emissions (Fig. 1C). As soon as possible after core recovery on the surface vessel, each was divided into aliquots for different analyses. The pushcores were horizontally sectioned into 1-cm thick slices while surface layers of the blade cores were removed via siphon in horizontal half-cm layers. Our specimens were from the top 1 cm in pushcores and top 0.5-cm in blade cores. Blade core BLC18 was the source of foraminifers used in a feeding experiment previously described by Schmidt et al. (2022).

rDNA SEQUENCING

An aliquot of sediment was reserved for foraminiferal rDNA sequencing (DNA barcoding), from which cytoplasmbearing specimens were isolated at sea, allowed to air dry and then stored individually. Ashore, these specimens were mounted on SEM stubs, imaged with Scanning Electron Microscopy (SEM; Zeiss EVOLS10) at the SCIAM Facility of the University of Angers, and subsequently individually extracted for DNA with DOC (Deoxycholate) buffer (Pawlowski, 2000). Taxon-specific primers for foraminifera, s14F3-J2 and s14F1-N6 (Pawlowski, 2000; Darling et al., 2016), were used with two rounds of PCR following the protocol described in Darling et al. (2016). The amplified region (\sim 500 bp) is situated at the 3' end of the SSU rDNA and is used for foraminiferal barcoding (Pawlowski & Holzmann, 2014). Foraminiferal amplifications were sequenced with the Sanger method (GATC Biotech, Cologne) and deposited in GenBank under accession numbers MN514777 to MN514782 (Schmidt et al., 2022) and PP265051 - PP265060 (present study). To investigate the microbiome of foraminifera, primers 1380f and 1510r were used with the same for aminiferal DNA extracts to amplify a \sim 160-bp fragment in the V9 region of 18S rDNA (Amaral-Zettler et al., 2009). The 18S samples were processed with two successive PCR rounds as described in Schweizer et al. (2022). One negative control (no added DNA) was performed in parallel. All amplicons were pooled in equimolar concentrations, and the concentration of the pool was monitored with quantitative PCR (KAPA SYBR FAST, Merck). The equimolar pool was mixed with 5% of phiX phage mix and run on a MiSeq sequencing system (Illumina) with a MiSeq cartridge 300 v2. Library constructions, MiSeq sequencing and demultiplexing were performed on the ANAN platform (SFR QUASAV, INRAE Beaucouzé, France). Raw reads were de-multiplexed to samples with DADA2 v.1.6.0 (Callahan et al., 2016). MiSeq overhangs and primers were removed with Cutadapt v.3.5 (Martin, 2011). Sequence data were processed using DADA2 v. 1.16 (Callahan et al., 2016) in R (R-Core-Team, 2016), following the tutorial for paired-end data (https://benjjneb.github. io/dada2/tutorial.html). Raw reads were quality controlled by truncating the reads (forward and reverse length of 120 bp) and filtering to a maximum number of 'expected errors' of

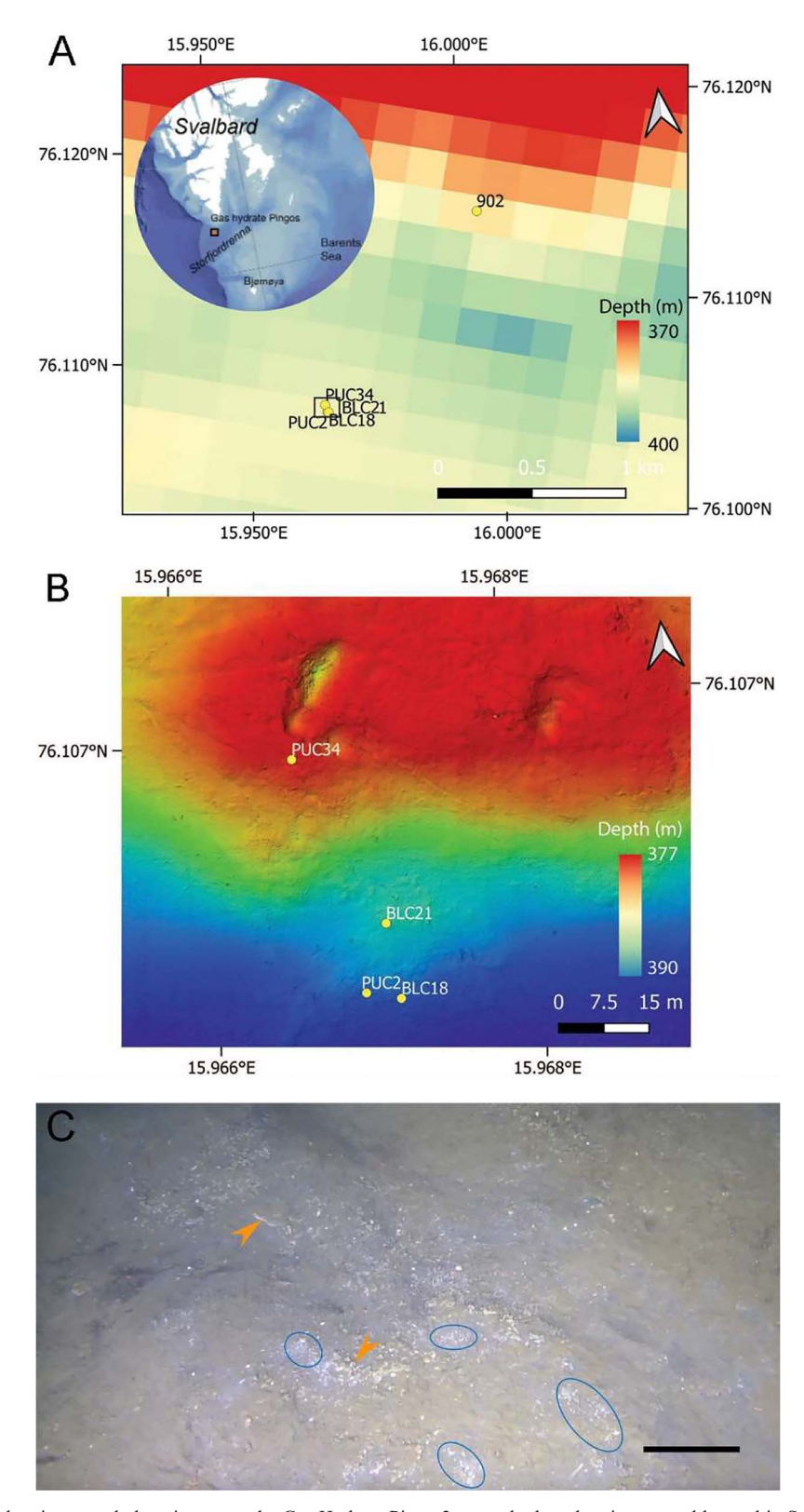


FIGURE 1. **A, B,** Maps showing sample locations near the Gas Hydrate Pingo 3, a gas-hydrate bearing mound located in Storfjordrenna, near Svalbard, Norway in the Arctic. **A,** Locator map showing sampling sites approximately 50 km south of Svalbard, in the Barents Sea (inset). **B,** Detailed bathymetric map showing four sampling sites, south of Gas Hydrate Pingo 3. **C,** Underwater photograph of general habitat of gas hydrate seep area. Blue ovals encircle representative microbial mats; orange arrowheads point to authigenic carbonate. Scale = \sim 50 cm.

Table 1. Number of specimens examined with TEM (n) for each species investigated, along with source core number(s), habitat cored plus organelles and other cellular components observed by species. M = mitochondrion, G = Golgi, P = peroxisome, EOB = electron opaque body, V = vacuole, L = lipid droplet, RB = residual body, DV = degradation vacuole, C = chloroplast, FV = fibrillar vesicle, N = nucleus, E1 = endobiont type 1, E2 = endobiont type 2. For organelles/structures, **bold** = **highly abundant**; italics = few.

Species	n	Core(s)	Habitat(s)	Organelles/structures observed
Elphidium clavatum	3	BLC18	control	M, G, <i>P</i> , EOB, V, L , <i>RB</i> , <i>DV</i> , C
Nonionellina labradorica	4	PUC2	seep	M, G, P, EOB, V, L, RB, FV, DV, C
Buccella sp.	4	BLC18, PUC2	3 control; 1 seep	M, G, P, EOB, V, L, RB, N, C
Robertina arctica	3	PUC2, PUC34	2 seep; 1 control	M, G, P, EOB, V, L, N, FV, C, E1, E2

two. Amplicon sequence variants (ASV) were dereplicated if identical, clustered, and pair-end reads merged using a minimum overlap of 12 bp and maximum mismatch of 0 bp. Chimeras were removed using the 'pooled' method (DADA2). The ASVs were taxonomically assigned using PR² v.4.12.0 (Guillou et al., 2013). HTS reads were deposited in the Sequence Read Archive (SRA) at NCBI (PRJNA1077881; https://www.ncbi.nlm.nih.gov/sra/PRJNA1077881). The phyloseq package (McMurdie & Holmes, 2013) on R was used to calculate relative abundances and diversity with the Shannon index (Shannon, 1948) for the foraminiferal microbiomes.

Cellular Ultrastructure

Specimens examined for cellular ultrastructure were different than those genetically analyzed because the two methods are incompatible. Shortly after core collection, sediment aliquots designated for cellular ultrastructure analyses by Transmission Electron Microscopy (TEM) were sieved using nested 500-, 250-, and 125-μm screens with *in situ* bottom water (2°C, salinity 35). From the 250–500-µm fraction, foraminifera with colored cytoplasm in most chambers were isolated using a fine picking brush and placed individually into microcentrifuge tubes containing chemical preservative (4% glutaraldehyde/ 2% paraformaldehyde) in Red Sea seawater (salinity 35; LeKieffre et al., 2018a). Samples were maintained at \sim 5°C during transport to the laboratory at the University of Angers, where isolated specimens were processed using our standard osmication and embedding methods (LeKieffre et al., 2018a) except that grids were stained using UranyLess® EM Stain (Electron Microscopy Sciences, USA). At the University of Angers' SCIAM facility, ultra-thin sections (70 nm) were observed and imaged with a JEOL JEM-1400 Transmission Electron Microscope. Specimen viability was determined by assessing organelle appearances and additional cellular attributes. During these analyses, we observed and recorded the presence and appearance of copious chloroplasts within four foraminiferal taxa: Buccella sp., Elphidium clavatum Cushman 1930, Nonionellina labradorica (Dawson 1850), and Robertina arctica d'Orbigny 1846 (Table 1).

In addition to the four species noted above, *Trifarina angulosa* (Williamson, 1858), *Globobulimina* sp., different cassidulinids, and unknown porcelaneous specimens were examined for their ultrastructure. None of these taxa exhibited (a) living individuals and/or (b) abundant intact chloroplasts in all conspecifics, so they are not discussed further in this contribution. Vitality is not always evident in foraminifera under light microscopy, so we used TEM to survey for vitality (i.e., living vs. dead) and cellular characteristics.

RESULTS

FORAMINIFERAL IDENTIFICATIONS

Twenty-nine specimens were imaged with SEM (Figs. A1, A2) and individually extracted for DNA. Among them, sixteen specimens gave sequences for DNA barcoding, and seven were investigated for their microbiome (Table 2). Because of limited resources, we did not analyze all specimens for their microbiome. All sequenced specimens were collected from outside the seep. Sequencing results indicate that the three Elphidium specimens (Figs. 2A, A1) belong to the S4 genetic type referred to the morphospecies Elphidium clavatum (Darling et al., 2016). The eight nonionids sequenced here were identified as Nonionellina labradorica (Figs. 2B, A2) plus one Nonionella species, of which the sequence is published here for the first time (Nonionella sp. in Fig. A1). One specimen morphologically recognized as Buccella frigida (Cushman, 1922) had a sequence identical to published sequences (ON087244-ON087248) from Svalbard and identified in GenBank as Buccella tenerrima (Brady 1950; Fig. 2C). Therefore, we prefer to identify this specimen as Buccella sp. until more taxonomic work combining morphological and molecular approaches is done on this genus. A robertinid identified morphologically as Robertina arctica was genetically similar to previously published sequences (EU672992, HE998677) identified as the same species (Fig. 2D). One Islandiella sp. and one Globobulimina auriculata (Bailey, 1851) were also sequenced (Fig. A1). The Islandiella sequence probably represents a different species from those already published in GenBank, whereas the Globobulimina

TABLE 2. Specimens successfully sequenced for DNA barcoding.

Species	Isolate number	Core	Accession number	Microbiome study
Elphidium clavatum	Bt055	BLC18	PP265051	yes
Elphidium clavatum	Bt056	BLC18	PP265052	yes
Elphidium clavatum	Bt057	BLC18	PP265053	yes
Buccella sp.	Bt058	BLC18	PP265054	yes
Nonionellina labradorica	Bt059	BLC18	MN514777	yes
Nonionellina labradorica	Bt061	BLC18	PP265055	no
Nonionellina labradorica	Bt062	BLC18	MN514778	no
Nonionellina labradorica	Bt063	BLC18	MN514779	yes
Robertina arctica	Bt064	BLC18	PP265056	yes
Globobulimina auriculata	Bt066	BLC18	PP265057	no
Nonionella digitata?	Bt068	BLC18	PP265058	no
Islandiella sp.	Bt070	BLC18	PP265059	no
Nonionellina labradorica	Bt071	BLC18	MN514780	no
Nonionellina labradorica	Bt072	BLC18	MN514781	no
Nonionellina labradorica	Bt073	BLC18	MN514782	no
Nonionellina labradorica	Bt079	BLC21	PP265060	no

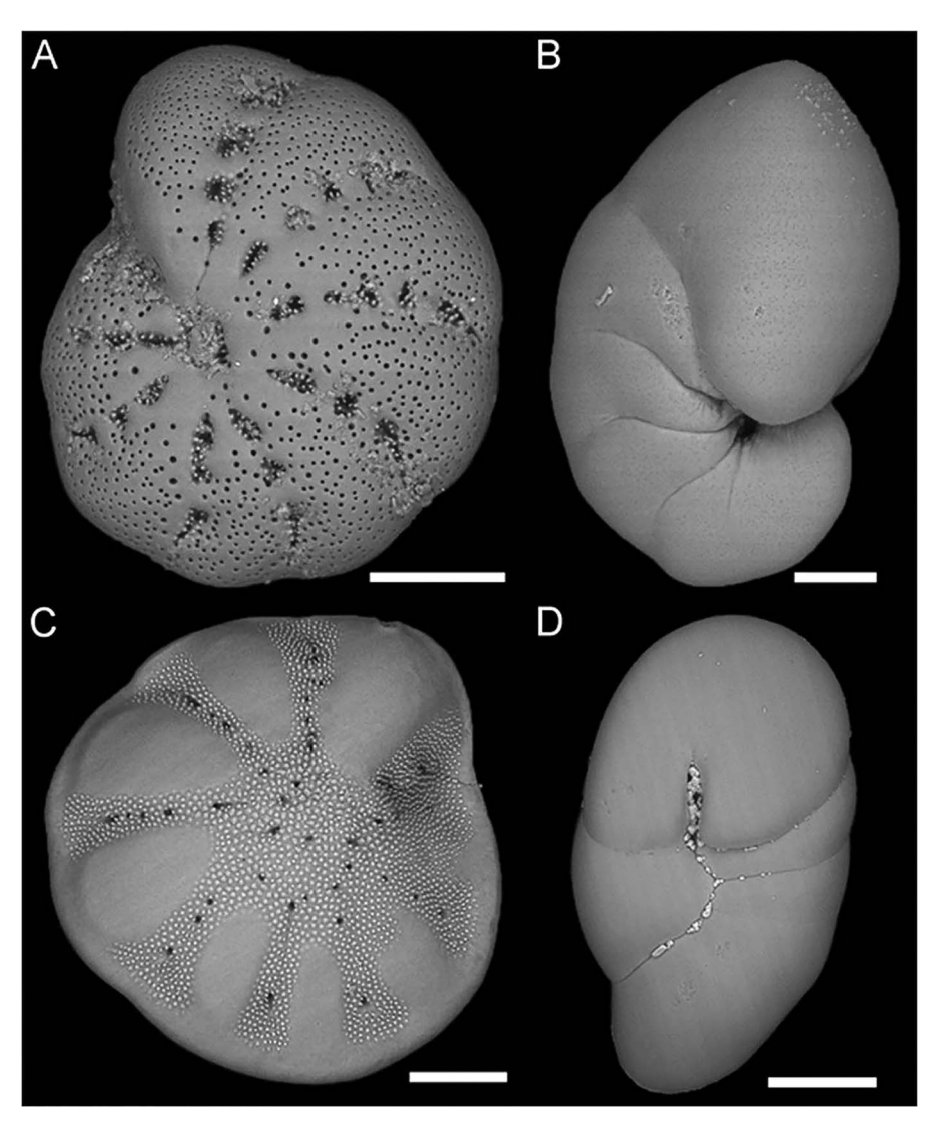


FIGURE 2. Scanning Electron Micrographs (SEMs) of the four benthic foraminiferal species investigated with Transmission Electron Microscopy (TEM). **A,** *Elphidium* S4, also denoted here as *Elphidium clavatum*; **B,** *Nonionellina labradorica*; **C,** *Buccella* sp.; **D,** *Robertina arctica*. Scales: A, C, D = 100 µm; B = 50 µm.

sequence is similar to previously sequenced congeners (MG800664-MG800665; ON818317-ON818320; ON818444).

FORAMINIFERAL ULTRASTRUCTURE

Because ROV-collected pushcores and blade cores have limited surface areas, our aliquots for TEM analyses did not always yield numerous conspecifics. We attempted to obtain conspecifics from both habitats (seep and non-seep control; Table 1). Cytoplasm-containing specimens of *Robertina arctica* and *Buccella* sp. were isolated from both habitats. However, the only *Elphidium clavatum* specimens with cytoplasm were exclusively from non-seep samples while the only *Nonionellina labradorica* with cytoplasm were from a pushcore with a white bacterial mat, associated with a methane emission site (Fig. 1C).

The three *Elphidium clavatum* examined for ultrastructure, all collected from outside the seep, had intact mitochondria (Figs. 3A–C). Additional well-preserved structures included Golgi apparatus (Fig. 3C), electron opaque bodies (Fig. 3C),

vacuoles (Fig. 3D), and lipid droplets (Fig. 3); only rarely were peroxisomes observed in these specimens. Residual bodies and degradation vacuoles were noted in moderate to low abundance (not shown). Each specimen had sequestered chloroplasts (Figs. 3B–D), often in high abundance (Fig. 3D). The chloroplasts appeared to be intact and well integrated into the foraminiferal cytoplasm (i.e., were not membrane-bound within degradation or food vacuoles).

All four *Nonionellina labradorica* individuals examined, exclusively from a white microbial mat associated with methane seepage, had intact mitochondria (Figs. 4A–D). Other well-preserved organelles included peroxisomes (Figs. 4A, D) and Golgi apparatus (Figs. 4B, D), as well as other features such as large vacuoles (Figs. 4B, C, E), fibrillar vesicles (Figs. 4A, D), electron opaque bodies (Figs. 4A–D), and lipid droplets (Figs. 4A–C). Degradation vacuoles were noted, although rather rare (not shown). Intact chloroplasts were also present in *N. labradorica* cytoplasm, sometimes abundantly (Fig. 4E) and also did not appear to be within food vacuoles.

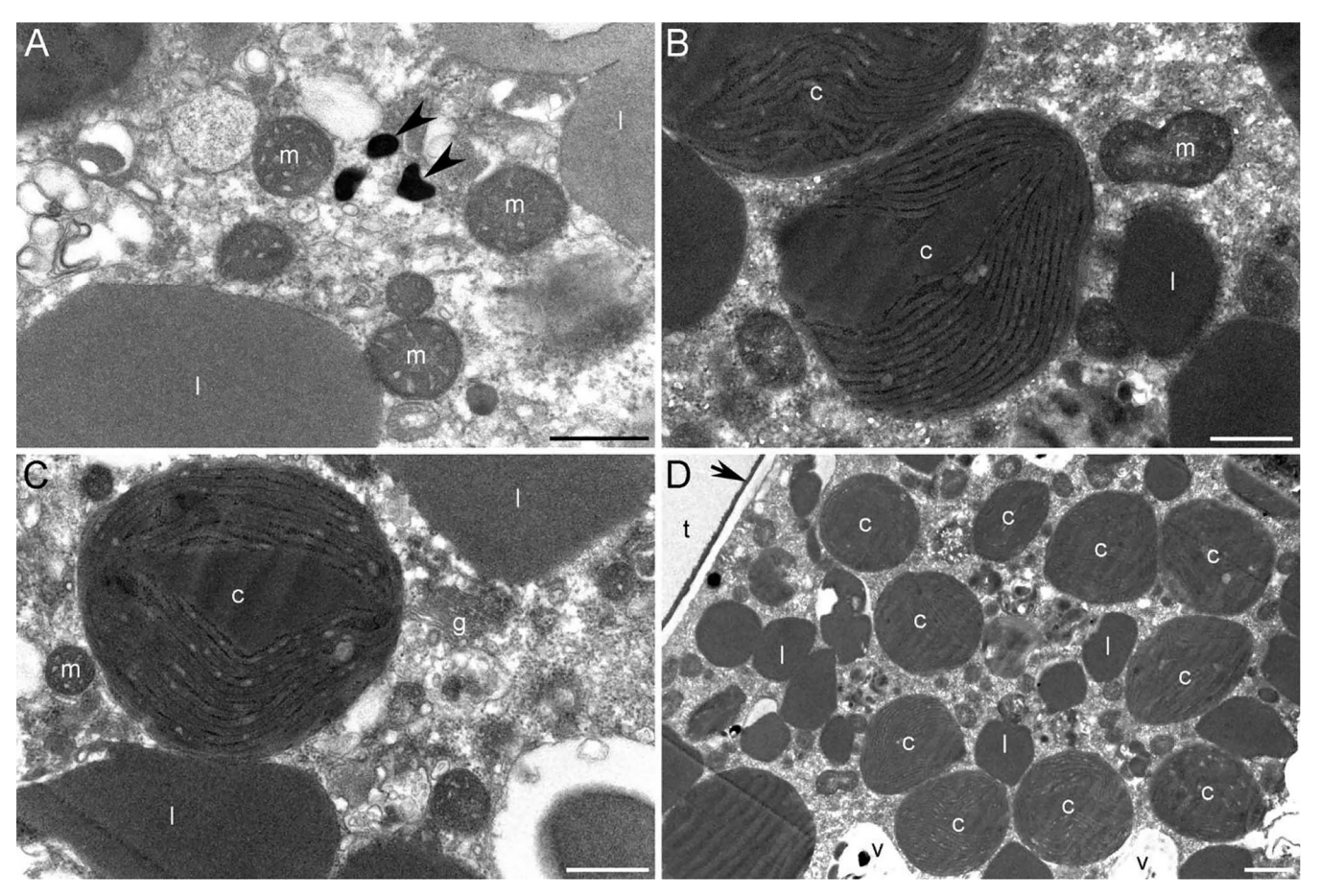


FIGURE 3. Cellular ultrastructure of *Elphidium clavatum* from non-seep core BLC18. **A,** Intact organelles: mitochondria (m), electron opaque bodies (arrowhead), lipid droplets (l). **B, C,** Additional intact features, including chloroplasts (c) and Golgi apparatus (g). **D,** Lower magnification view showing abundance of sequestered chloroplasts. Cell periphery (organic lining) is shown (arrow) and location of (decalcified) test denoted t. v = vacuoles. Scales: A–C = 0.5 μm; D = 1 μm.

Although cytoplasm-containing *N. labradorica* were absent in our non-seep samples, preventing us from assessing if non-seep specimens had kleptoplasts, Schmidt et al. (2022) has documented this phenomenon in other *N. labradorica* from the non-seep BLC18 sample.

All *Buccella* sp. specimens (n = 4) had intact mitochondria (Figs. 5A, B), Golgi apparatus (Fig. 5A), peroxisomes (Fig. 5B), lipid droplets (Fig. 5A), electron opaque bodies (Figs. 5A, D), and large vacuoles (Fig. 5F). We also documented a nucleus with nucleoli and a well-preserved nuclear envelope (Fig. 5C including inset) and residual bodies (Fig. 5D). Sequestered chloroplasts were intact and relatively abundant in *Buccella* sp. although the numerous large vacuoles occupied considerable cell volume that may have impacted the ability of this foraminifer to harbor more kleptoplasts (Fig. 5F). As in *Elphidium clavatum* and *Nonionellina labradorica*, the chloroplasts appeared to be well integrated in the cytoplasm of *Buccella* sp., not in food vacuoles.

The cellular ultrastructure of the sole *Robertina arctica* obtained from the non-seep core was highly deteriorated (not shown), indicating that the specimen had died long before collection. The cytoplasm of the other two specimens, both from seep sediments, exhibited better preservation (Fig. 6) including intact mitochondria (Figs. 6A, B),

Golgi apparatus (Fig. 6C), lipid droplets, fibrillar vesicles (Figs. 6B, G), and nucleus (Fig. 6E) suggesting these specimens were living at the time of collection. Their overall cytological appearance (Figs. 6F-I), however, was quite distinct from the ultrastructure of other species examined for this study. For example, these specimens had few peroxisomes, well-preserved large vacuoles, and electron opaque bodies but had features not noted in the other three species, including what appear to be two types of intracellular prokaryotes, hereafter denoted endobiont 1 (Fig. 6D) and endobiont 2 (Fig. 6E), both of which were bacilli-shaped prokaryotes. Both seep-associated Robertina arctica had both types of endobionts. Endobiont 1 could be relatively abundant (Figs. 6F, G). These two foraminifera had overall unorganized cytology (Figs. 6F-I) suggesting, perhaps, that they could have been dying while being overcome by the endobiont populations acting as parasites or scavengers (Bernhard et al., 2018). Chloroplasts were present (Figs. 6F-I) in R. arctica, in relatively high abundance (Fig. 6I); some of these chloroplasts appeared to be intact and outside any membrane-bound vacuoles (Figs. 6F, G) while others were in degradation vacuoles and appeared to be deteriorated (Figs. 6H, I). In some of these cases, additional cytological features such as lipid droplets were also included in the putative food vacuole (Fig. 6H).

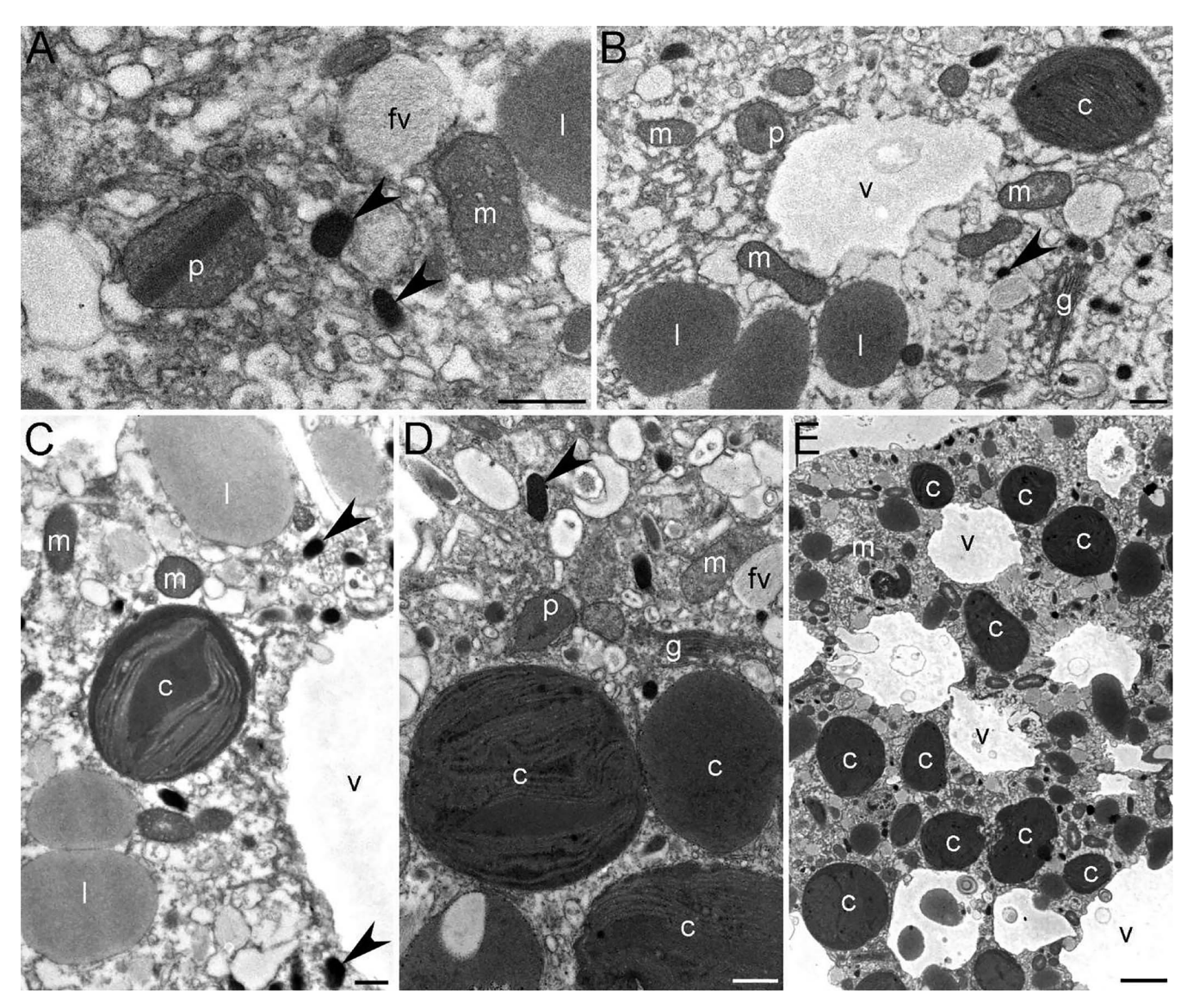


Figure 4. Cellular ultrastructure of three *Nonionellina labradorica* from seep core PUC2. **A**, Intact organelles: mitochondria (m), peroxisome (p), electron opaque bodies (arrowheads), fibrillar vesicles (fv), lipid droplets (l). **B–D**, Additional intact features include chloroplasts (c), Golgi apparatus (g), and vacuoles (v). **E**, Lower magnification view showing abundance of sequestered chloroplasts. Scales: A–D = 0.5 μm; E = 2 μm.

We note that because complete serial reconstructions were not made of any specimen, any assessment comparing kleptoplast abundance between individuals or species cannot be made.

KLEPTOPLAST ULTRASTRUCTURE

At the ultrastructural level, the chloroplasts within all foraminiferal cells examined for this study generally appeared similar in gross morphology across foraminifera taxa, with an outer lamella and single pyrenoid without any apparent transverse lamella (Fig. 5D). Some kleptoplasts included osmiophilic (electron-opaque or dark) globules (e.g., Fig. 5E; Jauffrais et al., 2018) while others had lighter, near white, vesicular-like structures (Fig. 3C), or both dark and light bodies (e.g., Figs. 6F–H). It is possible that some of the white structures indicated chloroplast degradation (Jauffrais et al., 2019a), but others could be intact vesicles (e.g., Fig. 6G; Lindquist et al., 2016). Unfortunately, the resolution of our micrographs is

insufficient to determine the number of stacked membranes within thylakoids, which can be useful for chloroplast-source identification purposes above Order level. Nevertheless, microbiome sequencing results provide some answers about the source of chloroplasts in these foraminifera.

KLEPTOPLAST IDENTIFICATIONS AND DIVERSITY

The three *Elphidium clavatum* (Bt55, Bt56, Bt57) sequenced for their microbiome gave 42,472, 2,832, and 324 18S reads, respectively. The phylum Ochrophyta (mostly represented by diatoms in this study) totaled nearly 70% of the sequence reads for *E. clavatum* 18S (Fig. 7A). The three *Nonionellina labradorica* (Bt59, Bt62, Bt63) sequenced for their microbiome gave 34,028, 0, and 270 reads, respectively. The phylum Ochrophyta totaled almost 100% of the reads for *N. labradorica* 18S (Fig. 7A). Within the diatoms, the most representation was from Thalassiosirales (88.8%) and *Porosira* (10.9%; Fig. 7C). As

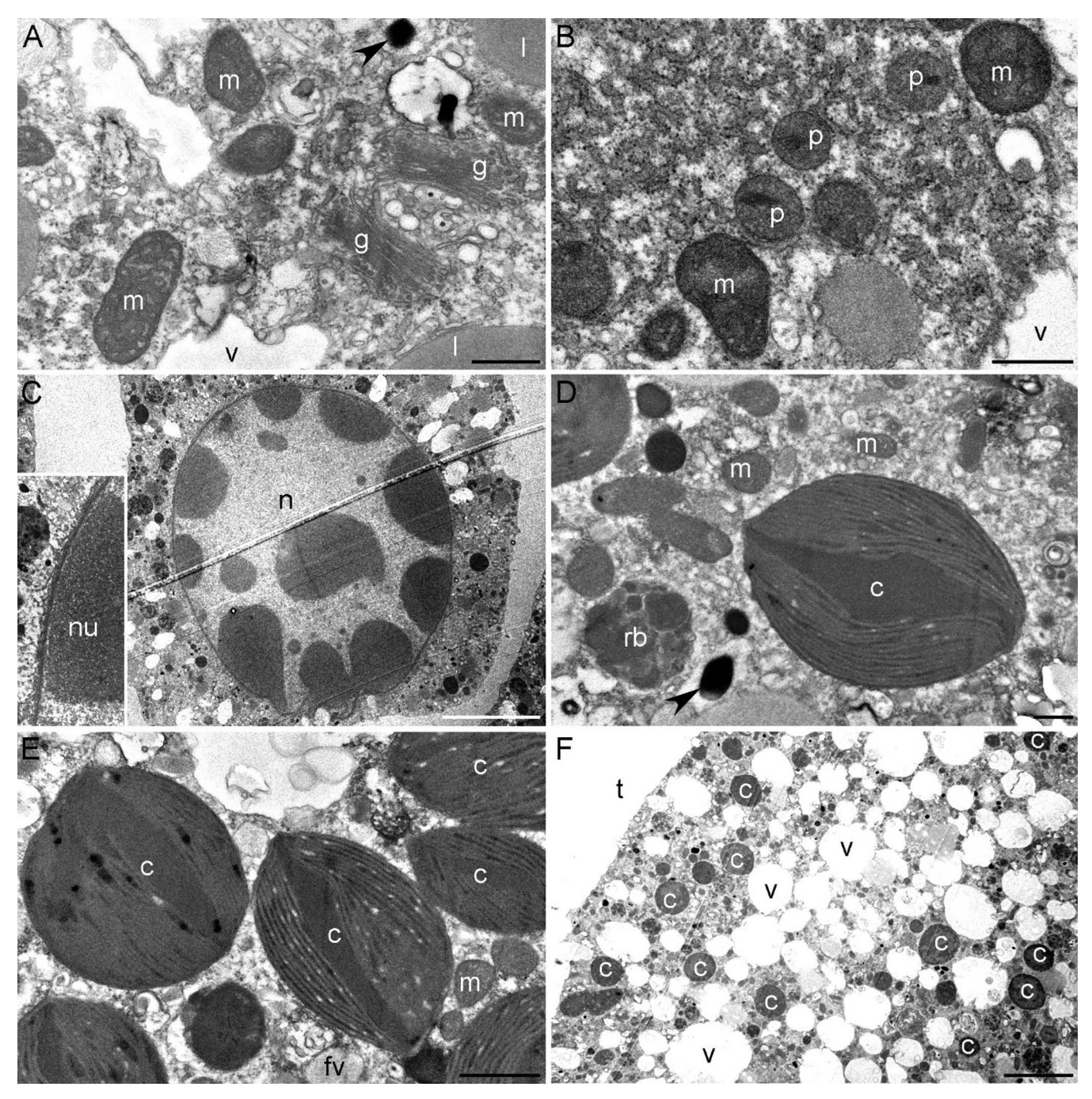


FIGURE 5. Cellular ultrastructure of *Buccella* sp. A, Intact organelles: mitochondria (m), Golgi apparatus (g), electron opaque bodies (arrowheads), lipid droplets (l), vacuoles (v). B, C, Additional intact features, including peroxisomes (p) and nucleus (n) with nucleoli (nu). Inset in c: nuclear envelope. D, E, Sequestered chloroplasts (c) among mitochondria, electron opaque bodies, residual body (rb), and fibrillar vesicles (fv). F, Lower magnification view showing the abundance of sequestered chloroplasts and large vacuoles (v). Location of (decalcified) test denoted t. A–C from seep specimen (PUC2); D–F from non-seep specimen (BLC18). Scales: A, B, D = $0.5 \mu m$; C = $10 \mu m$; E = $1 \mu m$; F = $5 \mu m$.

different genera belonging to Thalassiosirales (e.g., *Thalassiosira* and *Skeletonema*) share the same sequence for this region of 18S, it was not possible to identify them below Order. One *Buccella* sp. (Bt58) was sequenced for its microbiome; it gave 37 reads, which is too low to be statistically representative. No Ochrophyta was recognized in Bt58 18S, but reads mostly belonged to unclassified Eukaryotes, Metazoa, and Ciliophora (Fig. 7A). Unsurprisingly (because of the low number of reads), the

microbiome diversity of *Buccella* sp. was very low with the Shannon index (H') below 0.5 (Fig. 7B). The sole *Robertina arctica* (Bt64) sequenced for its 18S microbiome yielded 34,229 reads, with Metazoa being the most represented taxon with \sim 55% of the reads, while Ochrophyta totaled \sim 28% and Dinoflagellata \sim 12% (Fig. 7A). The microbiome diversity of *R. arctica* was the highest observed in this study (H' = 5; Fig. 7B). Although 81% of the diatom reads belonged to

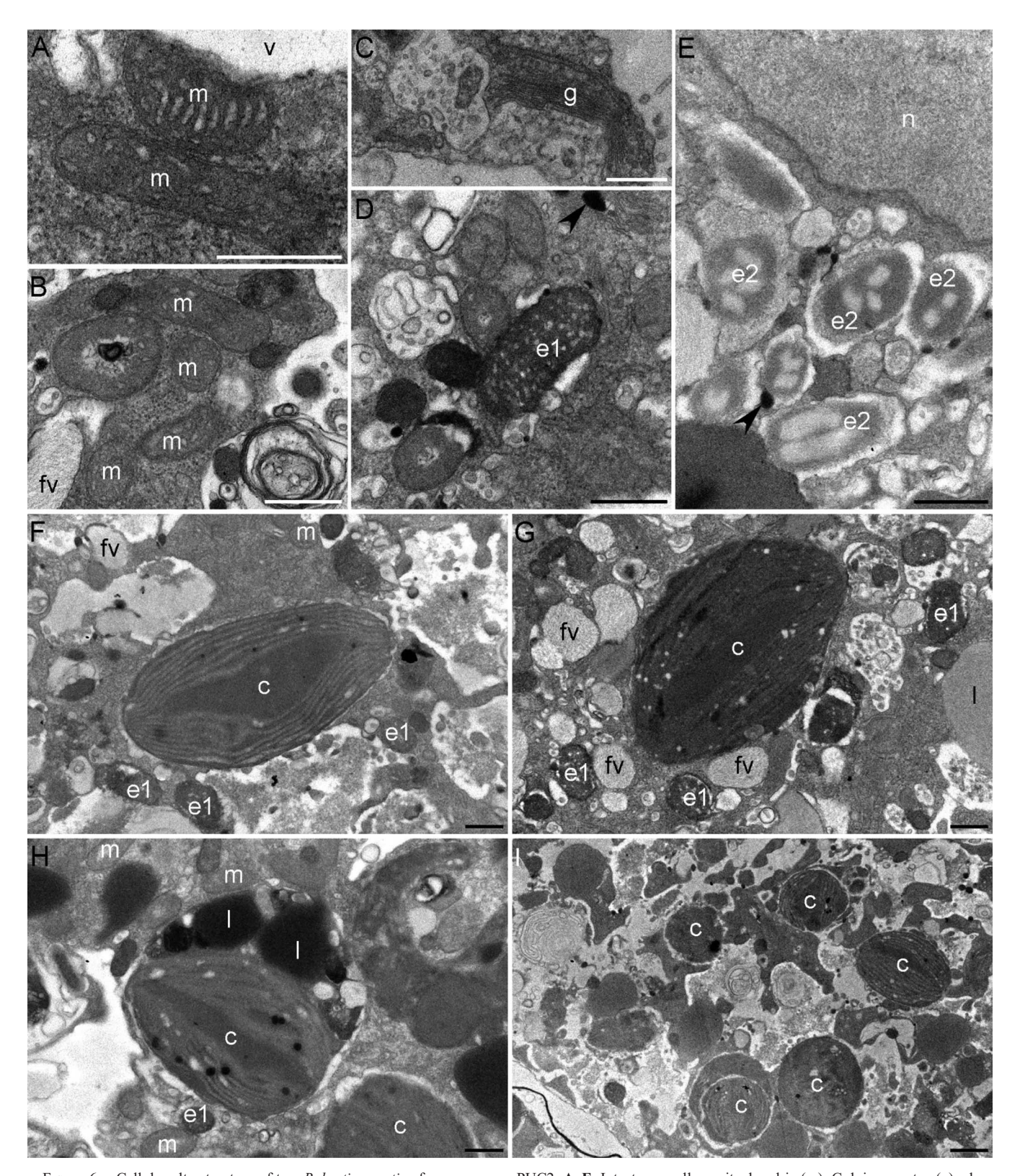


FIGURE 6. Cellular ultrastructure of two *Robertina arctica* from seep core PUC2. **A–E**, Intact organelles: mitochondria (m), Golgi apparatus (g), electron opaque bodies (arrowheads), nucleus (n), and fibrillar vesicles (fv). Note two types of bacteria-like endobionts (e1, e2) in D and E. **F**, **G**, Sequestered chloroplasts (c) among ruptured vacuoles and generally unorganized cytoplasm. **H**, Sequestered chloroplasts with additional entities (e.g., lipid droplets) in membrane-bound vacuole. **I**, Lower magnification view showing abundance of sequestered chloroplasts among generally unorganized cytoplasm. Scales: $A-H=0.5~\mu m$; $I=1~\mu m$.

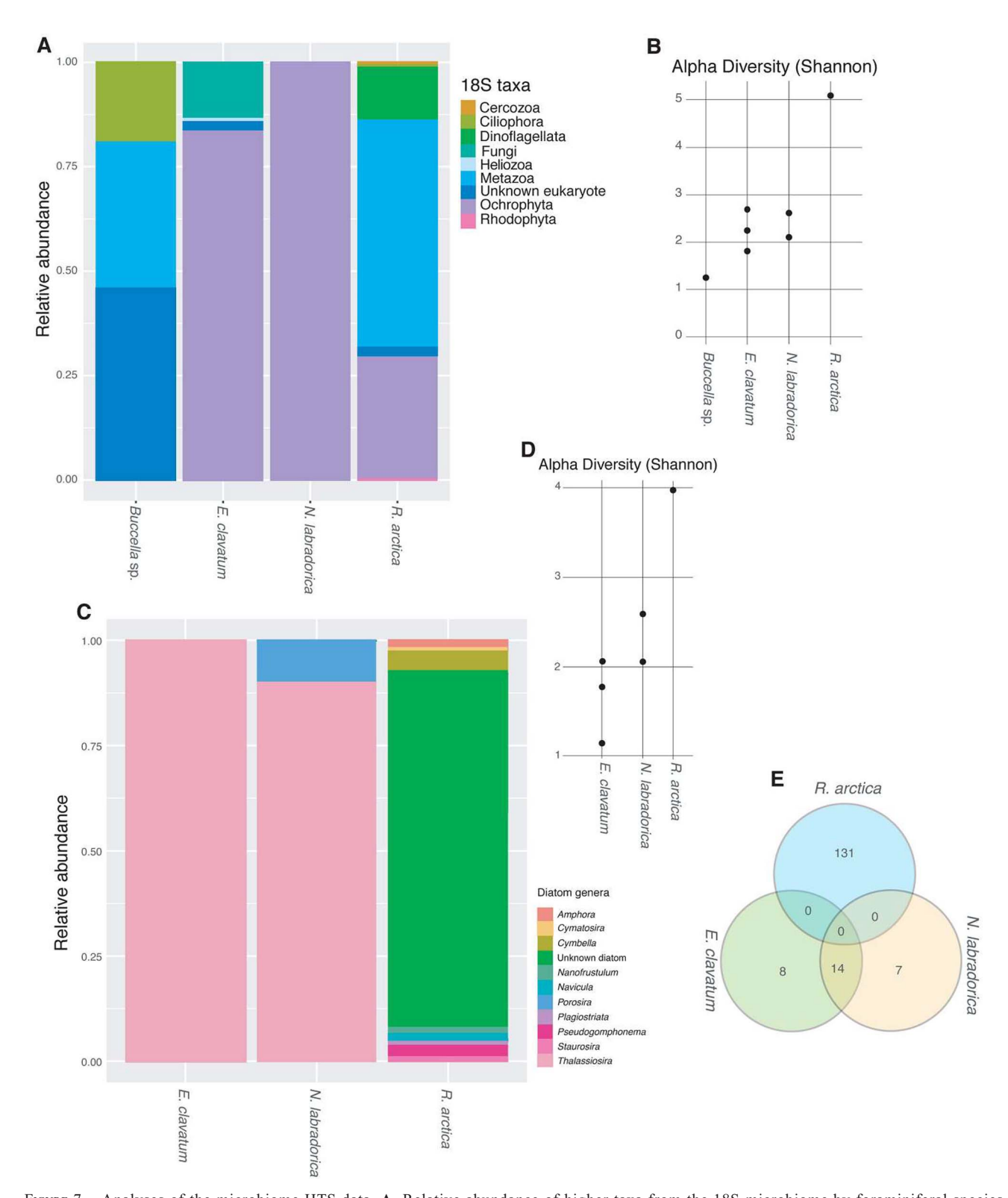


FIGURE 7. Analyses of the microbiome HTS data. **A**, Relative abundance of higher taxa from the 18S microbiome by foraminiferal species. **B**, Shannon index of the different replicates grouped by foraminiferal species to show total 18S diversity of the microbiome. **C**, Relative abundance of diatom genera from the 18S microbiome by foraminiferal species. **D**, Shannon index of the different replicates grouped by foraminiferal species to show diatom 18S diversity of the microbiome. **E**, Venn diagram showing the ASVs shared between *E. clavatum*, *N. labradorica*, and *R. arctica*.

unidentified taxa (Fig. 7C), diatom diversity was still very high (H' = 4; Fig. 7D).

The taxon diversity within the *Elphidium clavatum* microbiomes (expressed as the Shannon index) was similar to that of the *Nonionellina labradorica* microbiomes (H' roughly between 2 and 3), but lower than those within *Robertina arctica* (Fig. 7B). Within diatoms, the order Thalassiosirales was the most represented with more than 99% of the reads (Fig. 7C). The diatom diversity was lower in *E. clavatum* (H' between 0.25 and 2.1) than in *N. labradorica* and *R. arctica* (Fig. 7D). The three *E. clavatum* specimens shared 14 diatom ASVs with the two *N. labradorica* specimens, but none with the *R. arctica* specimen (Fig. 7E).

DISCUSSION

FORAMINIFERAL VIABILITY

Establishing viability in benthic foraminifera can be a challenge (Bernhard, 2000); cellular ultrastructural analysis via TEM is one means to assess viability. Mitochondria with clear double membranes and cristae are typically used as a viability indicator (Nomaki et al., 2016), especially if additional organelles also appear to be well preserved (Bernhard et al., 2001). Importantly, it is not expected that each mitochondrion has visible intact double membranes and clear cristae because those sectioned near their ends or edges will appear less distinct due to their structure or geometry.

The mitochondria of each taxon included well-preserved examples plus other typical organelles such as Golgi apparatus, peroxisomes, and, in some cases, nuclei, in addition to typical foraminiferal structures such as lipid droplets, large "empty" vacuoles, fibrillar vesicles, and electron opaque bodies (LeKieffre et al., 2018a). The peroxisomes in our specimens were not noted to be abundant nor coupled with endoplasmic reticulum, as noted for many benthic foraminifera from environments with low concentrations of dissolved oxygen (e.g., Bernhard & Bowser, 2008; Bernhard et al., 2010). The lack of a nucleus in each specimen is not unexpected as resources prohibited the complete serial sectioning and examination of each individual in totality.

KLEPTOPLAST MORPHOLOGICAL ATTRIBUTES

In addition to the well-preserved organelles, chloroplasts were noted in each specimen discussed in this contribution other than the single highly degraded non-seep *Robertina arctica* that was deemed dead and only briefly examined. Generally, these sequestered chloroplasts were integrated into the foraminiferal host cytoplasm, rather than surrounded by a membrane like those of food vacuoles (i.e., degradation vacuoles of LeKieffre et al., 2018a). The exceptions were chloroplasts in the two seep-associated *R. arctica* specimens, where some of the plastids appeared to be membrane bound, often with other cytoplasmic structures (Figs. 7H, I). For these two individuals, we interpret the chloroplasts as being either kleptoplasts serving some function to the host or a food source.

The kleptoplasts noted in our specimens exhibited overall morphology similar to that of other foraminiferal kleptoplasts, which are known to be of diatom origin (Grzymski et al., 2002; Bernhard & Bowser, 2008; Pillet et al., 2011; Jauffrais et al., 2018). One considerable difference in kleptoplast morphology is that kleptoplasts in this study lacked a visible

central transverse lamella across the pyrenoid, which has been noted in other bona fide diatom chloroplasts of kleptoplastidic foraminifera (e.g., see Grzymski et al., 2002, fig. 1A). While some sectioning planes are inappropriate for viewing a central lamella, here, we did not note any central lamella, even in properly oriented chloroplasts. The pyrenoid of kleptoplasts in Swedish Fjord Nonionellina labradorica subject to experimentation also consistently lacked the transverse lamella (Jauffrais et al., 2019a), while kleptoplasts of different *Elphidium* taxa appeared to have pyrenoids both with and without a central lamella (e.g., figs. 6E, G, H in Jauffrais et al., 2018). However, despite the lack of transverse lamellae, 18S microbiome results showed that kleptoplasts have, most probably, a diatom origin in our Elphidium clavatum, N. labradorica and Robertina arctica specimens (Fig. 7). Establishing the role of kleptoplasts in foraminiferal biology is a burgeoning research topic (Jauffrais et al., 2016; LeKieffre et al., 2018c; Jauffrais et al., 2019b; Gomaa et al., 2021, 2025; Jesus et al., 2022; Powers et al., 2022; Pinko et al., 2023) that is raising many questions as observations are amassed.

Species-specific Observations

Three of our taxa—Nonionellina labradorica, Buccella sp., and Elphidium clavatum—are known to be relatively common in the Svalbard region of the Arctic (Skirbekk et al., 2016; Fossile et al., 2020). Many of the species of the widespread genus Elphidium are known to harbor chloroplasts, but these reports have been on populations collected from very shallow water depths such as mudflats at low tide or the rocky intertidal zone (Jauffrais et al., 2018; Jesus et al., 2022). To our knowledge, this is the first documented case of Elphidium kleptoplasty deduced from TEM from the lower continental shelf. The 18S microbiome of our E. clavatum, with a high percentage of diatom reads, is congruent with kleptoplastic activity.

It is well established that *Nonionellina labradorica* sequesters chloroplasts (Cedhagen, 1991; Jauffrais et al., 2019a; Schmidt et al., 2022), often at considerable water depths. For example, populations of N. labradorica collected as deep as 300 m off the Swedish west coast were shown to have sequestered chloroplasts (Cedhagen, 1991). While kleptoplast-bearing N. labradorica were reported in Schmidt et al. (2022), those specimens were obtained from BLC18, a core without a visible microbial mat at its surface, meaning it was not unequivocally from a hydrocarbon-seep microhabitat. The source of our N. labradorica specimens is a core that had a white bacterial mat at its sedimentwater interface, indicating active hydrocarbon emissions. Thus, this is the first well-documented case of kleptoplasty in a deepwater (~380 m) N. labradorica population associated with a hydrocarbon seep. The sequenced N. labradorica (sampled from BLC18), showed similarities with sequence data from Gullmar Fjord N. labradorica, as the percentage of diatoms was very high and the dominant diatoms were Thalassiosirales (Jauffrais et al., 2019a). Moreover, the microbiome of N. labradorica shared similarities with the sole E. clavatum from the same site: a high percentage of diatoms and a large amount of Thalassiosirales among which 14/21 ASVs of N. labradorica were shared with E. clavatum (Fig. 7E).

Among the different *Buccella* species, *Buccella frigida* is described by Murray (2006) as a taxon being locally dominant

in, for example, Russian estuaries and Svalbard fjords at water depths less than 100 m. In Saanich Inlet (British Columbia, Canada), B. frigida is a characteristic species between 10-31 m (Blais-Stevens & Patterson, 1998), occurring as deep as 90 m. Interestingly, a congener of Buccella [i.e., B. granulata (di Napoli Alliata, 1952), reported as B. frigida var. granulata] was documented from a shallow Adriatic seep (~25-m water depth: Panieri, 2006). However, because that study did not examine cell ultrastructure, kleptoplasty could not be ascertained in that population. Nevertheless, Buccella has been reported to live in deeper areas from Arctic zones such as the Storfjorden (Svalbard) at 120- and 160-m depth (Nardelli et al., 2023) and in the eastern Fram Strait at 1200-m depth (Dessandier et al., 2019). To our knowledge, this report is the first to document kleptoplasty in any *Buccella* species. Unfortunately, the low number of sequence reads could not allow any conclusion about our Buccella sp. microbiome but morphologically, the Buccella sp. kleptoplasts are similar to those of diatoms. Both habitats were represented in our Buccella sp. TEM-imaging efforts. As such, a comparison between microbial mat seep specimens and non-seep specimens did not reveal obvious differences, but as noted elsewhere, full serial reconstructions were not done, so a robust comparison is not possible.

The distribution of Robertina arctica is not well established. Two different species of robertinids are known from Norwegian waters between 128-801 m water depth (Mackensen et al., 1985) and from deeper than 1 km in Mediterranean waters (De Rijk et al., 1999). Robertina arctica is reported in low abundance in the Kongsfjorden at 35 m depth (Fossile et al., 2022). The genus is considered indicative of oligotrophy (O'Malley et al., 2021). The presence of intact mitochondria and other organelles in the two best preserved R. arctica suggests these specimens were living at the time of collection but the overall unorganized cytology and abundance of endobionts could be interpreted as indicators of cell death or imminent cell death. While endobionts are often considered putative symbionts, the endobionts could instead be parasites or scavengers (Bernhard et al., 2018) invading the foraminiferan cell, perhaps eventually causing its death. The sequenced R. arctica was also from the non-seep station (PUC34); it did not support a typical "kleptoplastic microbiome" as did Elphidium clavatum and Nonionellina labradorica, (i.e., a high number of diatom reads and no shared ASV with either other species; Fig. 7E). However, with only one specimen, it is difficult to conclusively infer generalities regarding the R. arctica microbiome.

Our data does not disqualify our *R. arctica* specimens as kleptoplasty candidates because individuals of known kleptoplastidic benthic foraminifera species can have microbiomes with 50% (GF366, Jauffrais et al., 2019b) or even less (0–40%; e.g., figs. 8, H19-10 in Schweizer et al., 2022) diatom reads. The relatively high abundance of metazoan ASVs (>50%; Fig. 7A) could indicate *Robertina* predation or scavenging on metazoans. This perspective gains some credence given that one of the main metazoan taxa detected in *Robertina* AVSs was Maxillopoda; consumption of crustaceans by foraminifera is well established (e.g., Bowser et al., 1992). While we did not note any metazoan tissue in our electron micrographs, we did not do complete serial sectioning, and

different specimens were sequenced *vs.* imaged for cytology. Regardless, metazoan predation/scavenging and kleptoplasty are not mutually exclusive. Our observations call for more microbiome data to investigate the potential kleptoplasty in *R. arctica*.

While we cannot definitively infer viability in our Robertina arctica, we can conclude that the seep-associated R. arctica was in the process of consuming chloroplasts while some appeared to be sequestered. Cedhagen (1991) noted that some of the chloroplasts sequestered by Nonionellina labradorica became degraded in winter, subsequently serving as a food source. A similar observation was made by Golikova et al. (2020) regarding subarctic saltmarsh Elphidium williamsoni. While our samples were collected before winter (i.e., in October), it is possible that the kleptoplasts confer a metabolic advantage to their foraminiferan host and also serve as a food source to that host. We believe this is the first report of kleptoplasty in aragonitic benthic foraminifera (see Blackmon & Todd, 1959, for mineralogy). Assuming that the two better-preserved individuals were viable, this is the first documented case of any living Robertininae in a hydrocarbon seep habitat, to our knowledge.

IMPORTANCE OF KLEPTOPLAST SOURCE

The foraminiferal microbiome seemed to be mainly of diatom origin as this was the most sequenced photosynthetic taxon in *Elphidium clavatum*, *Nonionellina labradorica*, and *Robertina arctica*. The low number of reads provided by *Buccella* sp. did not allow any conclusion regarding plastid source for this species.

A reason why diatoms are targeted by foraminifera for their kleptoplasts could be that they are always abundant in the microphytoplankton and they can sink fast when still alive (Agusti et al., 2015). Moreover, diatoms are well adapted to low light levels (Salmaso, 2003; Fisher & Halsey, 2016; Mou et al., 2022), and they could survive for some time when removed from the photic zone—if nitrate is available (Kamp et al., 2011)—despite the fact that it is not their natural environment. Thus, it is understandable that benthic foraminifera from habitats with low light levels or darkness should source their kleptoplasts from diatoms. Although it seems only the diatom chloroplast is maintained by the host foraminifer, diatom nuclear DNA is also well preserved in the foraminifers, as indicated by our sequencing results.

At our sampling area, the base of the euphotic zone is, at most, 75 m deep (Hill et al., 2013), depending on many parameters such as season and concentration of suspended inorganics and phytoplankton in the water column. A small proportion of sunlight penetrates deeper than the base of the euphotic zone (i.e., 1% PAR or photosynthetically active radiation; Wu et al., 2021), so it is a challenge to determine the water depth where sunlight ceases to penetrate. Recent reports note that even one photon can initiate the process of photosynthesis (Li et al., 2023). Although we sampled the top half to one cm of sediment, we know that at least one of our species (*N. labradorica*) typically has "deep infaunal" distributions (Fontanier et al., 2014). Living in sediments (below the sediment-water interface) must also filter photons, if present. In

sum, while we are quite confident that the light levels on the seafloor in our sampling area were very low and that at least some of these foraminifera are infaunal, we cannot definitively conclude there was complete darkness (i.e., complete lack of photons) and that photosynthesis was not occurring.

The role of kleptoplasts in N. labradorica from relatively deep water (\sim 70 m, Gullmar Fjord, Sweden) where little to no sunlight penetrates is not fully understood (Jauffrais et al., 2019a). No enrichment or uptake of inorganic carbon was noted in those populations exposed to sunlight or darkness. Thus, photosynthesis is inactive or is an insignificant metabolic pathway in those kleptoplastidic foraminifera. However, those Gullmar Fjord Nonionellina labradorica assimilated ammonium and sulfate (Jauffrais et al., 2019a), aiding cellular growth. These processes, however, were not necessarily linked to the kleptoplasts. A close relative of N. labradorica, Nonionella stella, collected from even deeper water depths (>550 m), was demonstrated to express genes to perform at least one anaerobic energy-producing metabolic pathway in their kleptoplasts (Gomaa et al., 2021). Given diatom pigments were the dominant algal pigment in benthic foraminifera from >4 km water depth (Cedhagen et al., 2014), it is plausible that kleptoplasty could be of importance at abyssal depths. While kleptoplasty was not discussed by those authors, their observations provide motivation for future searches for kleptoplastidic abyssal benthic foraminifera. Further dedicated studies are required to resolve the metabolic pathways in kleptoplastidic foraminifera from both sunlit and dark, aerobic and anoxic habitats.

(PALEO) ECOLOGICAL IMPLICATIONS

Benthic foraminiferal kleptoplasty has been linked to particular test (shell) ornamentation (Bernhard & Bowser, 1999), including the fossettes of *Elphidium* and apertural teeth in *N. labradorica*. The two taxa newly described as kleptoplastidic foraminifers also display ornamentation that could promote chloroplast isolation. *Buccella* sp. has fine pustules on its umbilical side (Fig. 2C). *Robertina arctica* can also have pustular ornamentation (see plate 3, figs. 20–23 in Scott & Vilks, 1991). Such morphological features have been used as kleptoplasty proxies to infer depositional environment from the foraminiferal fossil record (e.g., Meilijson et al., 2015).

The previously suggested link between benthic foraminiferal kleptoplasty and low-oxygen to anoxic habitats (Bernhard & Bowser, 1999) is not fully supported by our current observations nor observations of mudflat habitats (Cesbron et al., 2016), as only some of the kleptoplastidic foraminifera in this study were recovered from microbial mats indicative of the oxic-anoxic interface. It is possible that the foraminifers collected from non-seep settings either were living in existing sub-surface low-oxygen microhabitats or that they created their own low-oxygen microhabitat via, for example, sediment accumulation such as a cyst (Heinz et al., 2005). Micron- to millimeter-scale environmental investigations (Choquel et al., 2021; Jesus et al., 2023) combined with ultrastructural cytological analyses (Bernhard et al., 2023) and sediment biogeochemistry may help resolve these unknowns.

We assert that kleptoplasty may be even more widespread in benthic foraminifera but the prevalent use of Rose Bengal to distinguish between those foraminifera that were living and those that were dead at the time of collection may mask the phenomenon to many observers. Using an alternative viability indicator such as CellTracker Green CMFDA (Bernhard et al., 2006) or other fluorescence approaches (Frontalini et al., 2019) in combination with ultrastructural analysis may reveal even more cases of foraminiferal kleptoplasty.

CONCLUSIONS

Results demonstrate that the cytoplasm of four relatively common species of benthic foraminifera included intact chloroplasts despite living in water depths exceeding 375 m on the Arctic shelf. This is the first report of kleptoplasty for *Buccella* sp. and the aragonitic *Robertina arctica*. Because the available *R. arctica* had somewhat degraded cytoplasm, we cannot definitively establish their vitality but can establish their kleptoplastidic nature as well as what may be their dietary use of chloroplasts.

There was no universal correlation between kleptoplasty and environmental condition, meaning the kleptoplastidic foraminifers occurred in both seep-associated and control (non-seep) settings. Prior reports have noted sequestered chloroplasts in many Elphidium species, but deep-water kleptoplastidic Elphidium clavatum are documented here for the first time, to our knowledge. Nonionellina labradorica has also been previously noted to sequester chloroplasts, but we add seep-associated microbial mat to the known habitats of kleptoplastidic N. labradorica. Observations suggest that kleptoplasty is more widespread in foraminifera than previously thought, occurs in high-latitude deep-water foraminiferal populations, and occurs in at least one aragonite-bearing benthic foraminiferal species. Our deep-shelf kleptoplastidic benthic foraminiferal populations occur where light levels are very low to absent, bringing into question the role of these kleptoplasts; the chloroplast conundrum continues.

ACKNOWLEDGMENTS

We thank the Captain and crew of the R/V Kronprins Haakon, ROV Ægir team, and Science Party of KH cruise 18-05; Florence Manero, Hélène Roberge, Romain Mallet, and Rodolphe Perrot (SCIAM microscopy facility, Univ Angers) for their TEM and SEM expertise; Sophie Quinchard (LPG) for molecular analyses; Claudio Argentino (UiT) for assistance with cruise data access, and Coralie Marais, Muriel Bahut, and Sandrine Balzergue at the IRHS (Institut de Recherche en Horticulture et Semences, Angers) for performing the HTS run. We also thank Associate Editor J. Pawlowski and two anonymous reviewers for their helpful comments on an earlier version of this contribution. Funded by AKMA (Advancing Knowledge in Methane in the Arctic, project 287869), CAGE, Center for Arctic gas Hydrate Environment and Climate (project number 223259), NORCRUST (255150), and the French program Make Our Planet Great Again. CS was partly supported by DFG Individual Grant No. SCHM 3395/3-1. JMB was partially supported by US NSF 1634469, NASA 80NSSC21K0478, WHOI's Investment in Science Program, and the Région Pays de la Loire through the FRESCO Project.

REFERENCES

- Agusti, S., González-Gordillo, J. I., Vaqué, D., Estrada, M., Cerezo, M. I., Salazar, G., Gasol, J. M., and Duarte, C. M., 2015, Ubiquitous healthy diatoms in the deep sea confirm deep carbon injection by the biological pump: Nature Communications v. 6, DOI: 10.1038/ncomms8608.
- Amaral-Zettler, L. A., McCliment, E. A., Ducklow, H. W., and Huse, S. M., 2009, A method for studying protistan diversity using massively parallel sequencing of V9 hypervariable regions of small-subunit ribosomal RNA genes: Plos One, v. 4, DOI: 10.1371/journal.pone.0006372.
- Angeles, I. B., Argentino, C., Cermakova, K., Holzmann, M., Pawlowski, J., and Panieri, G., 2025, Sediment eDNA metabarcoding reveals the endemism in benthic foraminifera from Arctic methane cold seepages: ISME Communications, DOI: 10.1093/ismeco/ycaf058.
- Bernhard, J. M., 2000, Distinguishing live from dead foraminifera: Methods review and proper applications: Micropaleontology, v. 46, p. 38–46.
- Bernhard, J. M., and Bowser, S. S., 1999, Benthic foraminifera of dysoxic sediments: Chloroplast sequestration and functional morphology: Earth-Science Reviews, v. 46, p. 149–165.
- Bernhard, J. M., and Bowser, S. S., 2008, Peroxisome proliferation in foraminifera inhabiting the chemocline: An adaptation to reactive oxygen species exposure? Journal of Eukaryotic Microbiology, v. 55, p. 135–144, DOI: 10.1111/j.1550-7408.2008.00318.x.
- Bernhard, J. M., and Geslin, E., 2018, Introduction to the special issue entitled "Benthic Foraminiferal Ultrastructure Studies": Marine Micropaleontology, v. 138, p. 1–11.
- Bernhard, J. M., Sen Gupta, B. K., and Borne, P. F., 1997, Benthic foraminiferal proxy to estimate dysoxic bottom-water oxygen concentrations: Santa Barbara Basin, US Pacific continental margin: Journal of Foraminiferal Research, v. 27, p. 301–310.
- Bernhard, J. M., Buck, K. R., and Barry, J. P., 2001, Monterey Bay cold-seep biota: Assemblages, abundance, and ultrastructure of living foraminifera: Deep-Sea Research I, v. 48, p. 2233–2249.
- Bernhard, J. M., Ostermann, D. R., Williams, D. S., and Blanks, J. K., 2006, Comparison of two methods to identify live benthic foraminifera: A test between Rose Bengal and CellTracker Green with implications for stable isotope paleoreconstructions: Paleoceanography, v. 21, DOI: 10.1029/2006pa001290.
- Bernhard, J. M., Martin, J. B., and Rathburn, A. E., 2010, Combined carbonate carbon isotopic and cellular ultrastructural studies of individual benthic foraminifera: 2. Toward an understanding of apparent disequilibrium in hydrocarbon seeps: Paleoceanography, v. 25, DOI: 10.1029/2010pa001930.
- Bernhard, J. M., Tsuchiya, M., and Nomaki, H., 2018, Ultrastructural observations on prokaryotic associates of benthic foraminifera: Food, mutualistic symbionts, or parasites? Marine Micropaleontology, v. 138, p. 33–45, DOI: 10.1016/j.marmicro.2017.09.001.
- Bernhard, J. M., Nomaki, H., Shiratori, T., Elmendorf, A., Yabuki, A., Kimoto, K., Tsuchiya, M., and Shimanaga, M., 2023, Hydrothermal vent chimney-base sediments as unique habitat for meiobenthos and nanobenthos: Observations on millimeter-scale distributions: Frontiers in Marine Science, v. 9, DOI: 10.3389/fmars.2022.1033381.
- Blackmon, P. D., and Todd, R., 1959, Mineralogy of some foraminifera as related to their classification and ecology: Journal of Paleontology, v. 33, p. 1–15.
- Blais-Stevens, A., and Patterson, R. T., 1998, Environmental indicator potential of foraminifera from Saanich Inlet, Vancouver, Island, British Columbia, Canada: Journal of Foraminiferal Research, v. 28, p. 201–219.
- Bowser, S. S., Alexander, S. P., Stockton, W. L., and Delaca, T. E., 1992, Extracellular matrix augments mechanical properties of pseudopodia in the carnivorous foraminiferan *Astrammina rara* Role in prey capture: Journal of Protozoology, v. 39, p.724–732, DOI: 10.1111/j.1550-7408.1992.tb04455.x.
- Bünz, S., Vadakkepuliyambatta, S., Serov, P., Lepland, A., Himmler, T., Hong, W.-L., Lindgren, M., Moser, M., Jansson, P., Ferre, B., Svenning, M., Dimitri, K., Carrier, V., Geslin, E., Schmidt, C., Lucchi, R., and Mattingsdal, R., 2022, CAGE18-5 Cruise report: Remotelyoperated vehicle (ROV) investigations of active gas seepage sites in the Barents Sea: CAGE – Centre for Arctic Gas Hydrate, Environment and Climate Report Series, v. 6, DOI: 10.7557/cage.6853.
- Callahan, B. J., Mcmurdie, P. J., Rosen, M. J., Han, A. W., Johnson, A. J. A., and Holmes, S. P., 2016, DADA2: High-resolution sample

- inference from Illumina amplicon data: Nature Methods, v. 13, p. 581–583, DOI: 10.1038/nmeth.3869.
- Carrier, V., Svenning, M. M., Gründger, F., Niemann, H., Dessandier, P.-A., Panieri, G., and Kalenitchenko, D., 2020, The impact of methane on microbial communities at marine Arctic gas hydrate bearing sediment: Frontiers in Microbiology, v. 11, DOI: 10.3389/fmicb.2020.01932.
- Cartaxana, P., Rey, F., LeKieffre, C., Lopes, D., Hubas, C., Spangenberg, J. E., Escrig, S., Jesus, B., Caldado, G., Domingues, R., Kuhl, M., Calado, R., Meibom, A., and Cruz, S., 2021, Photosynthesis from stolen chloroplasts can support sea slug reproductive fitness: Proceedings of the Royal Society B-Biological Sciences, v. 288, DOI: 10.1098/rspb.2021.1779.
- Cedhagen, T., 1991, Retention of chloroplasts and bathymetric distribution in the sublittoral foraminiferan *Nonionellina labradorica*: Ophelia, v. 33, p. 17–30.
- Cedhagen, T., Cheah, W., Bracher, A., and Lejzerowicz, F., 2014, Algal pigments in Southern Ocean abyssal foraminiferans indicate pelagobenthic coupling: Deep Sea Research Part II: Topical Studies in Oceanography, v. 108, p. 27–32, DOI: 10.1016/j.dsr2.2014.07.017.
- Cesbron, F., Geslin, E., Jorissen, F. J., Delgard, M. L., Charrieau, L., Deflandre, B., Jezequel, D., Anschutz, P., and Metzger, E., 2016, Vertical distribution and respiration rates of benthic foraminifera: Contribution to aerobic remineralization in intertidal mudflats covered by *Zostera noltei* meadows: Estuarine, Coastal and Shelf Science, v. 179, p. 23–38, DOI: 10.1016/j.ecss.2015.12.005.
- Cesbron, F., Geslin, E., Le Kieffre, C., Jauffrais, T., Nardelli, M. P., Langlet, D., Mabilleau, G., Jorissen, F. J., Jézéquel, D., and Metzger, E., 2017, Sequestered chloroplasts in the benthic foraminifer *Hayne-sina germanica*: Cellular organization, oxygen fluxes and potential ecological implications: Journal of Foraminiferal Research, v. 47, p. 268–278, DOI: 10.2113/gsjfr.47.3.268.
- Choquel, C., Geslin, E., Metzger, E., Filipsson, H. L., Risgaard-Petersen, N., Launeau, P., Giraud, M., Jauffrais, T., Jesus, B., and Mouret, A., 2021, Denitrification by benthic foraminifera and their contribution to N-loss from a fjord environment: Biogeosciences, v. 18, p. 327–341, DOI: 10.5194/bg-18-327-2021.
- Darling, K. F., Schweizer, M., Knudsen, K. L., Evans, K. M., Bird, C., Roberts, A., Filipsson, H. L., Kim, J. H., Gudmundsson, G., Wade, C. M., Sayer, M. D. J., and Austin, W. E. N., 2016, The genetic diversity, phylogeography and morphology of Elphidiidae (Foraminifera) in the Northeast Atlantic: Marine Micropaleontology, v. 129, p. 1–23, DOI: 10.1016/j.marmicro.2016.09.001.
- De Rijk, S., Troelstra, S. R., and Rohling, E. J., 1999, Benthic foraminiferal distribution in the Mediterranean Sea: Journal of Foraminiferal Research, v. 29, p. 93–103, DOI: 10.2113/gsjfr.29.2.93.
- Dessandier, P.-A., Borrelli, C., Kalenitchenko, D., and Panieri, G., 2019, Benthic foraminifera in Arctic methane hydrate bearing sediments: Frontiers in Marine Science, v. 6, DOI: 10.3389/fmars.2019.00765.
- Dessandier, P.-A., Borrelli, C., Yao, H., Sauer, S., Hong, W.-L., and Panieri, G., 2020, Foraminiferal δ¹⁸O reveals gas hydrate dissociation in Arctic and North Atlantic Ocean sediments: Geo-Marine Letters, v. 40, p. 507–523, DOI: 10.1007/s00367-019-00635-6.
- El Bani Altuna, N., Rasmussen, T. L., Ezat, M. M., Vadakkepuliyambatta, S., Groeneveld, J., and Greaves, M., 2021, Deglacial bottom water warming intensified Arctic methane seepage in the NW Barents Sea: Communications Earth & Environment, v. 2, DOI: 10.1038/s43247-021-00264-x.
- Fisher, N. L., and Halsey, K. H., 2016, Mechanisms that increase the growth efficiency of diatoms in low light: Photosynthesis Research, v. 129, p. 183–197, DOI: 10.1007/s11120-016-0282-6.
- Fontanier, C., Duros, P., Toyofuku, T., Oguri, K., Koho, K. A., Buscail, R., Gremare, A., Radakovitch, O., Deflandre, B., De Nooijer, L. J., Bichon, S., Goubet, S., Ivanovsky, A., Chabaud, G., Menniti, C., Reichart, G. J., and Kitazato, H., 2014, Living (stained) deep-sea foraminifera off Hachinohe (NE Japan, Western Pacific): Environmental interplay in oxygen-depleted ecosystems: Journal of Foraminiferal Research, v. 44, p. 281–299.
- Fossile, E., Nardelli, M. P., Howa, H., Baltzer, A., Poprawski, Y., Baneschi, I., Doveri, M., and Mojtahid, M., 2022, Influence of modern environmental gradients on foraminiferal faunas in the inner Kongsfjorden (Svalbard): Marine Micropaleontology, v. 173, DOI: 10.1016/j. marmicro.2022.102117.

- Fossile, E., Nardelli, M. P., Jouini, A., Lansard, B., Pusceddu, A., Moccia, D., Michel, E., Péron, O., Howa, H., and Mojtahid, M., 2020, Benthic foraminifera as tracers of brine production in the Storfjorden "sea ice factory": Biogeosciences, v. 17, p. 1933–1953, DOI: 10.5194/bg-17-1933-2020.
- Frontalini, F., Losada, M. T., Toyofuku, T., Tyszka, J., Goleń, J., De Nooijer, L., Canonico, B., Cesarini, E., Nagai, Y., Bickmeyer, U., Ikuta, T., Tsubaki, R., Besteiro Rodriguez, C., Al-Enezi, E., Papa, S., Coccioni, R., Bijma, J., and Bernhard, J. M., 2019, Foraminiferal ultrastructure: A perspective from fluorescent and fluorogenic probes: Journal of Geophysical Research: Biogeosciences, v. 124, p. 2823–2850, DOI: 10.1029/2019JG005113.
- Golikova, E., Varfolomeeva, M., Yakovis, E., and Korsun, S., 2020, Saltmarsh foraminifera in the subarctic White Sea: Thrive in summer, endure in winter: Estuarine, Coastal and Shelf Science, v. 238, DOI: 10.1016/j.ecss.2020.106685.
- Gomaa, F., Utter, D. R., Powers, C., Beaudoin, D. J., Edgcomb, V. P., Filipsson, H. L., Hansel, C. M., Wankel, S. D., Zhang, Y., and Bernhard, J. M., 2021, Multiple integrated metabolic strategies allow foraminiferan protists to thrive in anoxic marine sediments: Science Advances, v. 7, DOI: 10.1126/sciadv.abf1586.
- Gomaa, F., Rogers, D. R., Utter, D. R., Powers, C., Huang, I.-T., Beaudoin, D. J., Zhang, Y., Cavanaugh, C., Edgcomb, V. P., and Bernhard, J. M., 2025, Array of metabolic pathways in a kleptoplastidic foraminiferan protist supports chemoautotrophy in dark, euxinic seafloor sediments: ISME Journal, v. 19, DOI: 10.1093/ismejo/wrae248.
- Gründger, F., Carrier, V., Svenning, M. M., Panieri, G., Vonnahme, T. R., Klasek, S., and Niemann, H., 2019, Methane-fuelled biofilms predominantly composed of methanotrophic ANME-1 in Arctic gas hydrate-related sediments: Scientific Reports, v. 9, DOI: 10.1038/s41598-019-46209-5.
- Grzymski, J., Schofield, O. M., Falkowski, P. G., and Bernhard, J. M., 2002, The function of plastids in the deep-sea benthic foraminifer, Nonionella stella: Limnology and Oceanography, v. 47, p. 1569–1580.
- Guillou, L., Bachar, D., Audic, S., Bass, D., Berney, C., Bittner, L., Boutte, C., Burgaud, G., De Vargas, C., Decelle, J., Del Campo, J., Dolan, J. R., Dunthorn, M., Edvardsen, B., Holzmann, M., Kooistra, W. H., Lara, E., Le Bescot, N., Logares, R., Mahé, F., Massana, R., Montresor, M., Morard, R., Not, F., Pawlowski, J., Probert, I., Sauvadet, A. L., Siano, R., Stoeck, T., Vaulot, D., Zimmermann, P., and Christen, R., 2013, The Protist Ribosomal Reference database (PR2): A catalog of unicellular eukaryote small subunit rRNA sequences with curated taxonomy: Nucleic Acids Research, v. 41, DOI: 10.1093/nar/gks1160.
- Hallock, P., 1999, Symbiont-bearing foraminifera, in Sen Gupta, B. K. (ed.), Modern Foraminifera: Kluwer, Dordrecht, p. 123–139.
- Heinz, P., Geslin, E., and Hemleben, C., 2005, Laboratory observations of benthic foraminiferal cysts: Marine Biology Research, v. 1, p. 149– 159, DOI: 10.1080/17451000510019114.
- Hill, V. J., Matrai, P. A., Olson, E., Suttles, S., Steele, M., Codispoti, L. A., and Zimmerman, R. C., 2013, Synthesis of integrated primary production in the Arctic Ocean: II. In situ and remotely sensed estimates: Progress in Oceanography, v. 110, p. 107–125, DOI: 10.1016/j.pocean.2012.11.005.
- Hong, W.-L., Torres, M. E., Carroll, J., Crémière, A., Panieri, G., Yao, H., Serov, P., 2017, Seepage from an arctic shallow marine gas hydrate reservoir is insensitive to momentary ocean warming: Nature Communications, v. 8, DOI: 10.1038/ncomms15745.
- Hong, W.-L., Torres, M. E., Portnov, A., Waage, M., Haley, B., and Lepland, A., 2018, Variations in gas and water pulses at an Arctic seep: Fluid sources and methane transport: Geophysical Research Letters, v. 45, p. 4153–4162, DOI: 10.1029/2018GL077309.
- Jauffrais, T., Jesus, B., Metzger, E., Mouget, J. L., Jorissen, F., and Geslin, E., 2016, Effect of light on photosynthetic efficiency of sequestered chloroplasts in intertidal benthic foraminifera (*Haynesina germanica* and *Ammonia tepida*): Biogeosciences, v. 13, p. 2715–2726, DOI: 10. 5194/bg-13-2715-2016.
- Jauffrais, T., Jesus, B., Méléder, V., and Geslin, E., 2017, Functional xanthophyll cycle and pigment content of a kleptoplastic benthic foraminifer: *Haynesina germanica*: Plos One, v. 12, DOI: 10.1371/journal. pone.0172678.
- Jauffrais, T., LeKieffre, C., Koho, K. A., Tsuchiya, M., Schweizer, M., Bernhard, J. M., Meibom, A., and Geslin, E., 2018, Ultrastructure and

- distribution of sequestered chloroplasts in benthic foraminifera from shallow-water (photic) habitats: Marine Micropaleontology, v. 138, p. 46–62.
- Jauffrais, T., LeKieffre, C., Schweizer, M., Geslin, E., Metzger, E., Bernhard, J. M., Jesus, B., Filipsson, H. L., Maire, O., and Meibom, A., 2019a, Kleptoplastic benthic foraminifera from aphotic habitats: Insights into assimilation of inorganic C, N and S studied with sub-cellular resolution: Environmental Microbiology, v. 21, p. 125–141.
- Jauffrais, T., LeKieffre, C., Schweizer, M., Jesus, B., Metzger, E., and Geslin, E., 2019b, Response of a kleptoplastidic foraminifer to heterotrophic starvation: Photosynthesis and lipid droplet biogenesis: FEMS Microbiology Ecology, v. 95, DOI: 10.1093/femsec/fiz046.
- Jesus, B., Ventura, P., and Calado, G., 2010, Behaviour and a functional xanthophyll cycle enhance photo-regulation mechanisms in the solarpowered sea slug *Elysia timida* (Risso, 1818): Journal of Experimental Marine Biology and Ecology, v. 395, p. 98–105, DOI: 10.1016/j. jembe.2010.08.021.
- Jesus, B., Jauffrais, T., Trampe, E. C. L., Goessling, J. W., LeKieffre, C., Meibom, A., Kühl, M., and Geslin, E., 2022, Kleptoplast distribution, photosynthetic efficiency and sequestration mechanisms in intertidal benthic foraminifera: ISME Journal, v. 16, p. 822–832.
- Jesus, B., Jauffrais, T., Trampe, E., Méléder, V., Ribeiro, L., Bernhard, J. M., Geslin, E., and Kühl, M., 2023, Microscale imaging sheds light on species-specific strategies for photo-regulation and photo-acclimation of microphytobenthic diatoms: Environmental Microbiology, v. 25, p. 3087–3103, DOI: 10.1111/1462-2920.16499.
- Johnson, M. D., Moeller, H. V., Paight, C., Kellogg, R. M., Mcilvin, M. R., Saito, M. A., and Lasek-Nesselquist, E., 2023, Functional control and metabolic integration of stolen organelles in a photosynthetic ciliate: Current Biology, v. 33, DOI: 10.1016/j.cub.2023.01.027.
- Kamp, A., De Beer, D., Nitsch, J. L., Lavik, G., and Stief, P., 2011, Diatoms respire nitrate to survive dark and anoxic conditions: Proceedings of the National Academy of Sciences, v. 108, p. 5649–5654, DOI: 10. 1073/pnas.1015744108.
- Lee, J. J., 1995, Living sands: The symbiosis of protists and algae can provide good models for the study of host/symbiont interactions: BioScience, v. 45, p. 252–261, DOI: 10.2307/1312418.
- LeKieffre, C., Bernhard, J. M., Mabilleau, G., Filipsson, H. L., Meibom, A., and Geslin, E., 2018a, An overview of cellular ultrastructure in benthic foraminifera: New observations in the context of existing literature: Marine Micropaleontology, v. 138, p. 12–32, DOI: 10.1016/j. marmicro.2017.10.005.
- LeKieffre, C., Jauffrais, T., Geslin, E., Jesus, B., Bernhard, J. M., Giovani, M. E., and Meibom, A., 2018b, Inorganic carbon and nitrogen assimilation in cellular compartments of a benthic kleptoplastic foraminifer: Scientific Reports, v. 8, DOI: 10.1038/s41598-018-28455-1.
- LeKieffre, C., Spero, H. J., Russell, A. D., Fehrenbacher, J. S., Geslin, E., and Meibom, A., 2018c, Assimilation, translocation, and utilization of carbon between photosynthetic symbiotic dinoflagellates and their planktic foraminifera host: Marine Biology, v. 165, DOI: 10.1007/s00227-018-3362-7
- Li, Q., Orcutt, K., Cook, R. L., Sabines-Chesterking, J., Tong, A. L., Schlau-Cohen, G. S., Zhang, X., Fleming, G. R., and Whaley, K. B., 2023, Single-photon absorption and emission from a natural photosynthetic complex: Nature, v. 619, p. 300–304, DOI: 10.1038/s41586-023-06121-5.
- Lindquist, E., Solymosi, K., and Aronsson, H., 2016, Vesicles are persistent features of different plastids: Traffic, v. 17, p. 1125–1138, DOI: 10.1111/tra.12427.
- Lopez, E., 1979, Algal chloroplasts in the protoplasm of three species of benthic foraminifera: Taxonomic affinity, viability and persistence: Marine Biology, v. 53, p. 201–211, DOI: 10.1007/bf00952427.
- Mackensen, A., Sejrup, H. P., and Jansen, E., 1985, The distribution of living benthic foraminifera on the continental slope and rise off southwest Norway: Marine Micropaleontology, v. 9, p. 275–306, DOI: 10.1016/0377-8398(85)90001-5.
- Martin, M., 2011, Cutadapt removes adapter sequences from high-throughput sequencing reads: EMBnet.journal, v. 17, p. 10–12, DOI: 10. 14806/ej.17.1.200.
- McMurdie, P. J., and Holmes, S., 2013, Phyloseq: An R Package for reproducible interactive analysis and graphics of microbiome census data: PLoS One, v. 8, DOI: 10.1371/journal.pone.0061217.

- Meilijson, A., Ashckenazi-Polivoda, S., Illner, P., Alsenz, H., Speijer, R. P., Almogi-Labin, A., Feinstein, S., Püttmann, W., and Abramovich, S., 2015, Evidence for specific adaptations of fossil benthic foraminifera to anoxic–dysoxic environments: Paleobiology, v. 42, p. 77–97, DOI: 10.1017/pab.2015.31.
- Mou, S., Zhang, Z., Zhao, H., Nair, S., Li, Y., Xu, K., Tian, J., and Zhang, Y., 2022, A dark-tolerant diatom (*Chaetoceros*) cultured from the deep sea: Journal of Phycology, v. 58, p. 208–218, DOI: 10.1111/jpy.13240.
- Murray, J. W., 2006, Ecology and Applications of Benthic Foraminifera: Cambridge University Press, Cambridge, 426 p.
- Nardelli, M. P., Fossile, E., Péron, O., Howa, H., and Mojtahid, M., 2023, Early taphonomy of benthic foraminifera in Storfjorden 'sea-ice factory': The agglutinated/calcareous ratio as a proxy for brine persistence: Boreas, v. 52, p. 109–123, DOI: 10.1111/bor.12592.
- Nomaki, H., Bernhard, J. M., Ishida, A., Tsuchiya, M., Uematsu, K., Tame, A., Kitahashi, T., Takahata, N., Sano, Y., and Toyofuku, T., 2016, Intracellular isotope localization in Ammonia sp. (Foraminifera) of oxygen-depleted environments: Results of nitrate and sulfate labeling experiments: Frontiers in Microbiology, v. 7, DOI: 10.3389/fmicb.2016.00163.
- Norris, R. D., Turner, S. K., Hull, P. M., and Ridgwell, A., 2013, Marine ecosystem responses to Cenozoic global change: Science, v. 341, p. 492–498, DOI: 10.1126/science.1240543.
- O'Malley, B. J., Schwing, P. T., Martínez-Colón, M., Spezzaferri, S., Machain-Castillo, M. L., Larson, R. A., Brooks, G. R., Ruiz-Fernández, A. C., and Hollander, D. J., 2021, Development of a benthic foraminifera based marine biotic index (Foram-AMBI) for the Gulf of Mexico: A decision support tool: Ecological Indicators: v. 120, DOI: 10.1016/j.ecolind.2020.106916.
- Panieri, G., 2006, Foraminiferal response to an active methane seep environment: A case study from the Adriatic Sea: Marine Micropaleontology, v. 61, p. 116–130, DOI: 10.1016/j.marmicro.2006.05.008.
- Pawlowski, J., 2000, Introduction to the molecular systematics of foraminifera: Micropaleontology, v. 46, p. 1–12.
- Pawlowski, J., and Holzmann, M., 2014, A plea for DNA barcoding of foraminifera: Journal of Foraminiferal Research, v. 44, p. 62–67, DOI: 10.2113/gsjfr.44.1.62.
- Pillet, L., and Pawlowski, J., 2013, Transcriptome analysis of foraminiferan Elphidium margaritaceum questions the role of gene transfer in kleptoplastidy: Molecular Biology and Evolution, v. 30, p. 66–69.
- Pillet, L., De Vargas, C., and Pawlowski, J., 2011, Molecular identification of sequestered diatom chloroplasts and kleptoplastidy in foraminifera: Protist, v. 162, p. 394–404.
- Pinko, D., Abramovich, S., Rahav, E., Belkin, N., Rubin-Blum, M., Kucera, M., Morard, R., Holzmann, M., and Abdu, U., 2023, Shared ancestry of algal symbiosis and chloroplast sequestration in foraminifera: Science Advances, v. 9, DOI: 10.1126/sciadv.adi3401.
- Powers, C., Gomaa, F., Billings, E. B., Utter, D. R., Beaudoin, D. J., Hansel, C. M., Wankel, S. D., Zhang, Y., and Bernhard, J. M., 2022, Canonically aerobic marine microeukaryotic foraminifera express atypical peroxisomal and mitochondrial metabolism in hypoxia and anoxia: Frontiers in Marine Science, Section on Marine Molecular Biology and Ecology, v. 9, DOI: 10. 3389/fmars.2022.1010319.
- R-Core-Team, 2016, R: A Language and Environment for Statistical Computing: Vienna, Austria, accessed at www.R-project.org/.
- Salmaso, N., 2003, Life strategies, dominance patterns and mechanisms promoting species coexistence in phytoplankton communities along

- complex environmental gradients: Hydrobiologia, v. 502, p. 13–36, DOI: 10.1023/b:hydr.0000004267.64870.85.
- Schiebel, R., and Hemleben, C., 2017, Planktic Foraminifers in the Modern Ocean: Springer Berlin, 358 pp.
- Schmidt, C., Geslin, E., Bernhard, J. M., LeKieffre, C., Svenning, M. M., Roberge, H., Schweizer, M., and Panieri, G., 2022, Deposit-feeding of Nonionellina labradorica (foraminifera) from an Arctic methane seep site and possible association with a methanotroph: Biogeosciences, v. 19, p. 3897–3909, DOI: 10.5194/bg-19-3897-2022.
- Schweizer, M., Jauffrais, T., Choquel, C., Méléder, V., Quinchard, S., and Geslin, E., 2022, Trophic strategies of intertidal foraminifera explored with single-cell microbiome metabarcoding and morphological methods: What is on the menu? Ecology and Evolution, v. 12, DOI: 10.1002/ece3.9437.
- Scott, D. B., and Vilks, G., 1991, Benthic foraminifera in the surface sediments of the deep-sea Arctic Ocean: Journal of Foraminiferal Research, v. 21, p. 20–38, DOI: 10.2113/gsjfr.21.1.20.
- Shannon, C. E., 1948, A mathematical theory of communication: The Bell System Technical Journal, v. 27, p. 379–423, DOI: 10.1002/j.1538-7305.1948.tb01338.x.
- Skirbekk, K., Hald, M., Marchitto, T. M., Junttila, J., Klitgaard Kristensen, D., and Aagaard Sørensen, S., 2016, Benthic foraminiferal growth seasons implied from Mg/Ca-temperature correlations for three Arctic species: Geochemistry, Geophysics, Geosystems, v. 17, p. 4684–4704, DOI: 10.1002/2016GC006505.
- Stoecker, D. K., Johnson, M. D., De Vargas, C., and Not, F., 2009, Acquired phototrophy in aquatic protists: Aquatic Microbial Ecology, v. 57, p. 279–310.
- Takagi, H., Moriya, K., Ishimura, T., Suzuki, A., Kawahata, H., and Hirano, H., 2015, Exploring photosymbiotic ecology of planktic foraminifers from chamber-by-chamber isotopic history of individual foraminifers: Paleobiology, v. 41, p. 108–121.
- Van Steenkiste, N. W., Stephenson, I., Herranz, M., Husnik, F., Keeling, P. J., and Leander, B. S., 2019, A new case of kleptoplasty in animals: Marine flatworms steal functional plastids from diatoms: Science Advances, v. 5, DOI: 10.1126/sciadv.aaw4337.
- Wu, J., Lee, Z., Xie, Y., Goes, J., Shang, S., Marra, J. F., Lin, G., Yang, L., and Huang, B., 2021, Reconciling between optical and biological determinants of the euphotic zone depth: Journal of Geophysical Research: Oceans, v. 126, DOI: 10.1029/2020JC016874.
- Yao, H., Niemann, H., and Panieri, G., 2020, Multi-proxy approach to unravel methane emission history of an Arctic cold seep: Quaternary Science Reviews, v. 244, DOI: 10.1016/j.quascirev.2020.106490.

Received 14 October 2024 Accepted 12 July 2025

APPENDIX CAPTIONS

FIGURE A1. SEM images of miscellaneous foraminifers individually extracted for DNA with their isolate number and species name. Sequenced specimens are noted with "-DNA". The Appendix figures can be found linked to the online version of this article.

FIGURE A2. SEM images of the *Nonionellina labradorica* individually extracted for DNA with their isolate number. Sequenced specimens are noted with "-DNA".

